*Electrochemical and Solid-State Letters,* **13** (2) B8-B10 (2010)
1099-0062/2009/13(2)/B8/3/$28.00 © The Electrochemical Society

# High Temperature, Low Humidity Proton Exchange Membrane Based on an Inorganic–Organic Hybrid Structure

**Yongcheng Jin, Keisuke Fujiwara, and Takashi Hibino**[*,z]

*Graduate School of Environmental Studies, Nagoya University, Nagoya 464-8601, Japan*

A high temperature and low humidity composite membrane consisting of $Sn_{0.95}Al_{0.05}P_2O_7$ and sulfonated polystyrene-*b*-poly(ethylene/butylene)-*b*-polystyrene (sSEBS) as inorganic and organic materials, respectively, was prepared and characterized. A homogeneous distribution of the $Sn_{0.95}Al_{0.05}P_2O_7$ particles in the matrix was accomplished in the thickness range of 25–80 μm, providing an elongation at break above 400%, which is approximately two times higher than that for Nafion. Moreover, moderate proton conductivities of sSEBS improved proton transfer between the $Sn_{0.95}Al_{0.05}P_2O_7$ particles in the matrix, resulting in a proton conductivity of approximately 0.01 S $cm^{-1}$ at 130°C without any humidification, which is 3 or more orders of magnitude higher than that for Nafion under the same conditions.
 [DOI: 10.1149/1.3267848] 

Manuscript submitted August 20, 2009; revised manuscript received November 2, 2009. Published December 9, 2009.

Proton conductors capable of operating at intermediate temperatures (100–200°C) and low relative humidities (10% or less at each temperature) currently hold great interest because of their advantages over Nafion-type fluoropolymers that are conventionally used in proton exchange membrane fuel cells (PEMFCs).[1,2] Operating a fuel cell at elevated temperatures gives the anode catalyst a high tolerance to CO, eliminating the need for a CO-removal unit. Electrode reaction kinetics is enhanced, permitting low Pt loadings. Operating a fuel cell under unhumidified conditions obviates the need for a complicated humidity control system. Thus, proton-conducting materials that can satisfy the above criteria have been proposed, developed, and evaluated. In particular, recent research efforts have been increasingly centered on the design of anhydrous proton conductors because these materials do not require the presence of water as a charge carrier.[3-6]

More recently, various metal diphosphates ($MP_2O_7$, where M = Sn,[7-12] Ce,[13] and Zr [14,15]) have been reported to show good proton conductivity in the temperature range of 100–400°C under water-free conditions. These proton conductors have also been explored as electrolytes for high temperature PEMFCs. For example, a fuel cell with the $Sn_{0.9}In_{0.1}P_2O_7$ electrolyte exhibited a stable performance in low humidity conditions and at high CO concentrations.[16] Moreover, this fuel cell allowed for the use of alternative anodes instead of Pt [17] and showed good fuel flexibility, including dimethyl ether[18] and hydrocarbons.[19] However, the electrolyte membranes used in previous studies were prepared by merely pressing $Sn_{0.9}In_{0.1}P_2O_7$ powders into pellets due to the difficulty in preparing sintered compacts of this material. The synthesis of a dense and flexible electrolyte membrane is a crucial requirement for practical applications of this material.

One promising approach for meeting the above requirements is to form hybrids of inorganic and organic materials because they offer the possibility of improving the mechanical properties of various difficult-to-consolidate inorganic materials.[20-24] Optionally, if the polymer has acidic functions as proton sites, high proton transfer between clusters of the proton conductor in the matrix is also expected. In the present study, we attempted to design composite membranes based on $Sn_{0.95}Al_{0.05}P_2O_7$. As a preliminary experiment, $Sn_{0.95}Al_{0.05}P_2O_7$ powders were blended with the following polymers: sulfonated polystyrene-*b*-poly(ethylene/butylene)-*b*-polystyrene (sSEBS), polystyrene-*b*-poly(ethylene/butylene)-*b*-polystyrene (SEBS) or polystyrene-b-poly(ethylene/propylene)-b-polystyrene, maleic anhydride functionalized polystyrene-b-poly(ethylene/butylene)-b-polystyrene, and poly(vinylidene difluoride). From the aspects of the electrochemical and mechanical characteristics, sSEBS with a block copolymer structure, shown in Fig. 1,[25] was the best all-round binder among the tested polymers, wherein a 20 wt % sSEBS was determined to be optimum for maintaining both the proton conductivity and the tensile strength as high as possible. Thus, this study mainly focused on experimental results using 20 wt % sSEBS as the organic binder.

## Experimental

$Sn_{0.95}Al_{0.05}P_2O_7$ was prepared as follows: $SnO_2$ and $Al(OH)_3$ powders were mixed with 85% $H_3PO_4$ and ion-exchanged water and were held with stirring at 300°C until the mixture formed a high viscosity paste. The pastes were calcined in an alumina pot at 650°C for 2.5 h and then ground with a mortar and a pestle. For comparison with the composite membranes, the compound powders were pressed into pellets under a pressure of $2 \times 10^3$ kg $cm^{-2}$.

sSEBS (1g) (Kuraray Co. Ltd.) was dissolved into a mixture of 80 wt % toluene and 20 wt % *iso*-butanol. $Sn_{0.95}Al_{0.05}P_2O_7$ powder (4g) was added into the solution while stirring at room temperature until a homogeneous slurry was formed. After grinding with a ball mill, the slurry was cast onto a poly(ethylene terephthalate) substrate and then dried at 120°C in air for 4 h. Finally, the membrane was peeled off and was cut into test samples with the appropriate sizes.

The cross-sectional morphology and the crystalline structure of the membrane samples were analyzed using a scanning electron microscope (SEM) equipped with an energy dispersive X-ray (EDX) detector and an X-ray diffractometer (XRD), respectively. The elongation at break and the tensile strength of the membrane samples were measured using a universal testing machine at room temperature and were estimated by dividing the maximum load by the cross-sectional area of the composite membrane. AC conductivity measurements of the membrane samples were performed using two Au plates as electrodes in unhumidified air.

$H_2/O_2$ fuel cells were fabricated using the membrane samples as electrolytes. Both the anode and the cathode (area: 0.5 $cm^2$) consisted of Pt/C (BASF, Pt loading: 1 mg $cm^{-2}$), which was impregnated with $H_3PO_4$ and heated at 130°C in air for 6 h. The electrolyte membrane was sandwiched between the two electrodes and hot-pressed at 120°C. Unless otherwise stated, the current–voltage curves of the fuel cell were measured by supplying unhumidified $H_2$ and $O_2$ to the anode and the cathode, respectively, at flow rates of 30 mL $min^{-1}$.

## Results and Discussion

A photograph of a thin $Sn_{0.95}Al_{0.05}P_2O_7$–sSEBS composite membrane prepared in this study is shown in Fig. 2a. The thickness of this composite membrane could be controlled from 25 to 80 μm. Although the distribution of $Sn_{0.95}Al_{0.05}P_2O_7$ in the matrix is difficult to estimate from this photograph, homogeneity ranging from several micrometers to a few tens of micrometers was established, as will be described later. The mechanical profile of this composite membrane is shown in Fig. 2b. A large elongation at break, above

* Electrochemical Society Active Member.
z E-mail: hibino@urban.env.nagoya-u.ac.jp

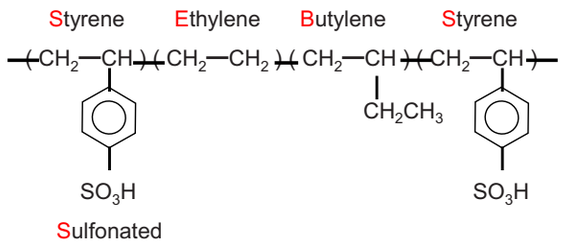


**Figure 1.** (Color online) Chemical structure of sSEBS.

400%, was obtained at a membrane thickness of 50 μm, which is superior to the values of 200–300% reported for Nafion.[26,27] Here, similar properties were observed in the thickness range of 25–80 μm, showing excellent extensibility control over the membrane thickness. The tensile strength of this composite membrane was measured to be 2.8 MPa, which is less than the value of about 10 MPa measured for Nafion; however, this composite membrane was sufficiently strong, allowing it to be fabricated into membrane electrode assemblies (MEAs).

The morphological and structural analyses of the $Sn_{0.95}Al_{0.05}P_2O_7$–sSEBS were carried out by SEM/EDX and XRD, respectively. As shown in Fig. 3a, SEM and EDX images revealed a homogeneous dispersion of $Sn_{0.95}Al_{0.05}P_2O_7$ particles throughout the cross section of the composite. The XRD pattern of this composite membrane sample was almost perfectly identical to that of the pure $Sn_{0.95}Al_{0.05}P_2O_7$ powder sample, indicating no influence of the present blending process on the crystalline structure of $Sn_{0.95}Al_{0.05}P_2O_7$. To obtain information about other physiochemical properties, a $H_2/O_2$ fuel cell was fabricated using this composite membrane as an electrolyte. As shown in Fig. 3b, the open-circuit voltages (OCVs) were always independent of the membrane thickness, meaning that both $H_2$ and $O_2$ crossover through the composite membrane was negligible. Figure 3b also gives additional information indicating that the ohmic resistance of the composite membrane decreased almost linearly with decreasing thickness and reached a minimum of approximately 0.5 Ω $cm^2$ at a thickness of 36 μm, which is an indirect evidence of the homogeneous distribution of $Sn_{0.95}Al_{0.05}P_2O_7$ in the matrix at the ~10 μm level.

The proton conductivity of the $Sn_{0.95}Al_{0.05}P_2O_7$–sSEBS composite membrane was compared with those of the individual materials and Nafion at various temperatures under unhumidified conditions. As shown in Fig. 4, in the temperature range of −20°C to room temperature, the proton conductivity of the composite membrane was as high as that of the pure $Sn_{0.95}Al_{0.05}P_2O_7$ pellet. This can be understood by the relatively high proton conductivity of sSEBS under such conditions. However, at elevated temperatures, the proton conductivity of the composite membrane was lower than that of the pure $Sn_{0.95}Al_{0.05}P_2O_7$ pellet. This is not surprising because sSEBS is no longer a good proton conductor under such conditions. More importantly, the proton conductivity of the composite membrane was reduced by using unsulfonated SEBS in place of sSEBS at temperatures below 200°C, whereas the opposite relationship was observed at temperatures above 200°C. Given the structural similarity of the two polymers, this difference observed below 200°C can be ascribed to the $-SO_3H$ groups available for proton transfer. The $-SO_3H$ group likely forms a proton-conducting pathway from one

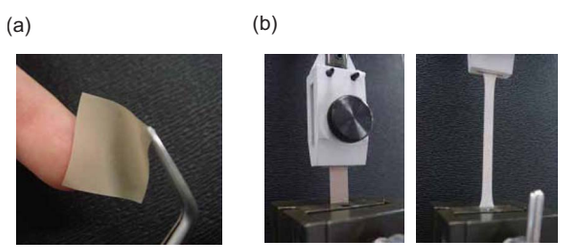


**Figure 2.** (Color online) Photographs of the (a) as-prepared composite membrane (thickness, 50 μm) and the (b) composite membrane before and after stretching (thickness, 50 μm).

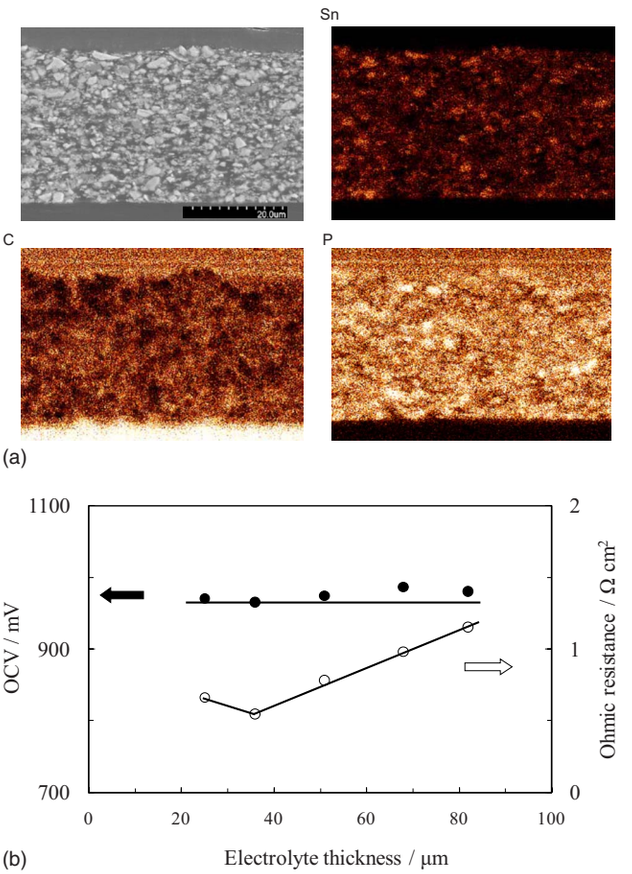


**Figure 3.** (Color online) Morphological and physiochemical observations of the composite membrane. (a) SEM image and Sn, P, and C element mappings; (b) OCV and ohmic resistance as a function of electrolyte thickness. In the fuel cell, unhumidified $H_2$ and $O_2$ were supplied to the anode and cathode chambers, respectively, at 150°C.

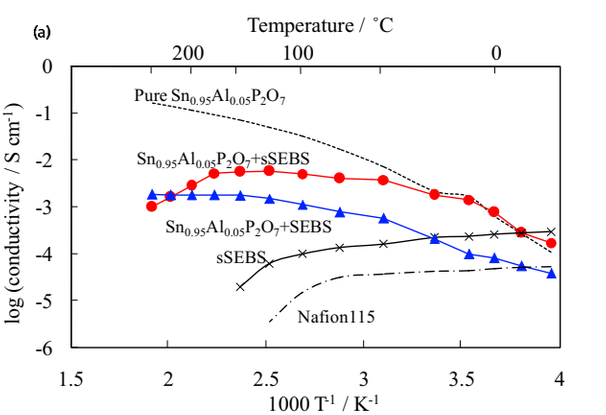


**Figure 4.** (Color online) The conductivity of various proton conductors from −20 to 250°C in unhumidified air ($pH_2O$ = 0.03 atm): $Sn_{0.95}Al_{0.05}P_2O_7$–sSEBS, $Sn_{0.95}Al_{0.05}P_2O_7$, sSEBS, $Sn_{0.95}Al_{0.05}P_2O_7$–SEBS, and Nafion 115.

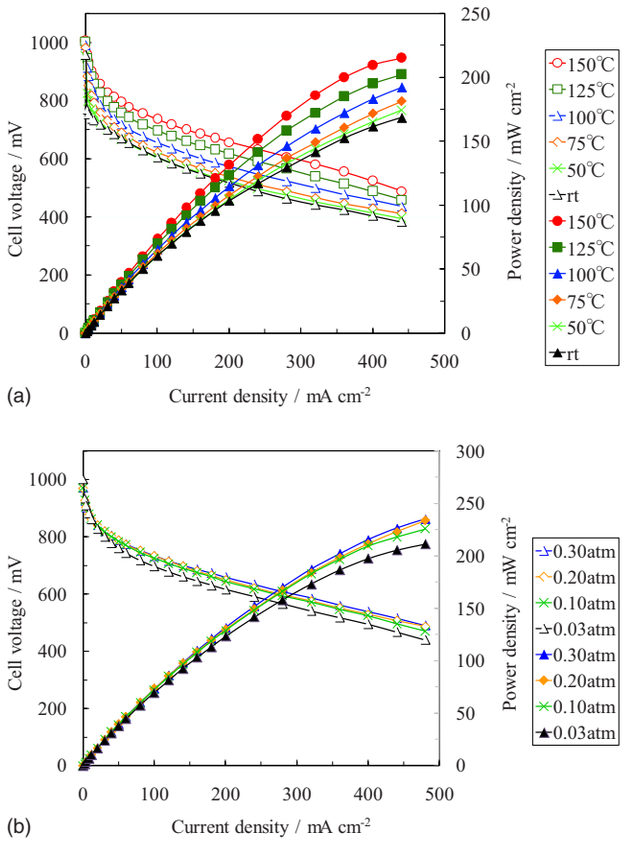


**Figure 5.** (Color online) Performance of a fuel cell with the composite membrane showing dependence of discharge properties (a) on the temperature in unhumidified conditions ($pH_2O$ = 0.03 atm) and (b) on $pH_2O$ at 150°C. In all cases, $H_2$ and $O_2$ were supplied to the anode and cathode chambers, respectively.

$Sn_{0.95}Al_{0.05}P_2O_7$ cluster to another. The $-SO_3H$ groups in many polymers were reported to be dehydrated or condensed above 200°C.[28-30] Thus, we can assume that the observations above 200°C are due to the decomposition of the $-SO_3H$ group and thereby probably the whole polymer structure, causing a large increase in the grain-boundary resistance in the matrix. In any event, the proton conductivities of this composite membrane from −20 to 130°C (the so-called glass transition temperature for Nafion)[31] are approximately 1–3 orders of magnitude higher than those measured for Nafion under the same conditions.

The cell performance was tested for a 50 μm thick composite membrane between room temperature and 150°C. As shown in Fig. 5a, the OCV exceeded 970 mV at all tested temperatures, and no limiting current behavior was observed at high current densities. The current–voltage slopes became lower as the operating temperature increased. Consequently, the power density at 450 mA $cm^{-2}$ was enhanced from 169 to 215 mW $cm^{-2}$ by increasing the temperature from room temperature to 150°C. The cell performance was also measured for the same MEA as above at various $pH_2O$ values. As shown in Fig. 5b, the fuel cell maintained high performance levels in the pressure range of 0.03–0.3 atm, proving a good performance at low-to-medium humidities. Here, the ohmic resistance of this composite membrane at each temperature and each $pH_2O$ was kept almost constant for at least 100 h, although it initially increased to some extent.

## Conclusion

In this study, we used sSEBS as an organic binder for $Sn_{0.95}Al_{0.05}P_2O_7$ because it is a polymer material with good thermal and chemical stabilities. Moreover, sSEBS itself shows a moderate proton conductivity of $10^{-4}$ or $10^{-5}$ S $cm^{-1}$ at intermediate temperatures, which is useful for proton transfer between $Sn_{0.95}Al_{0.05}P_2O_7$ particles in the matrix. A homogeneous distribution of $Sn_{0.95}Al_{0.05}P_2O_7$ in the matrix was accomplished in the thickness range of 25–80 μm, providing an elongation at break above 400% (approximately two times higher than that for Nafion) and a proton conductivity of approximately 0.01 S $cm^{-1}$ at 130°C without any humidification (3 orders of magnitude higher than that for Nafion). The resultant fuel cell generated OCVs of approximately 1000 mV and power densities of 200 mW $cm^{-2}$ or more between 100 and 150°C in unhumidified conditions.

*Nagoya University assisted in meeting the publication costs of this article.*

## References

1. Q. Li, R. He, J. O. Jensen, and N. J. Bjerrum, *Chem. Mater.*, **15**, 4896 (2003).
2. J. Zhang, Z. Xie, J. Zhang, Y. Tang, C. Song, T. Navessin, Z. Shi, D. Song, H. Wang, D. P. Wilkinson, et al., *J. Power Sources*, **160**, 872 (2006).
3. T. Uda, D. A. Boysen, and S. M. Haile, *Solid State Ionics*, **176**, 127 (2005).
4. T. Matsui, T. Kukino, R. Kikuchi, and K. Eguchi, *J. Electrochem. Soc.*, **153**, A339 (2006).
5. X. Chen, Z. Huang, and C. Xia, *Solid State Ionics*, **177**, 2413 (2006).
6. A. Matsuda, T. Kanzaki, K. Tadanaga, M. Tatsumisago, and T. Minami, *Solid State Ionics*, **154–155**, 687 (2002).
7. M. Nagao, A. Takeuchi, P. Heo, T. Hibino, M. Sano, and A. Tomita, *Electrochem. Solid-State Lett.*, **9**, A105 (2006).
8. M. Nagao, T. Kamiya, P. Heo, A. Tomita, T. Hibino, and M. Sano, *J. Electrochem. Soc.*, **153**, A1604 (2006).
9. X. Chen, C. Wang, E. A. Payzant, C. Xia, and D. Chu, *J. Electrochem. Soc.*, **155**, B1264 (2008).
10. A. Tomita, N. Kajiyama, T. Kamiya, M. Nagao, and T. Hibino, *J. Electrochem. Soc.*, **154**, B1265 (2007).
11. X. Wu, A. Verma, and K. Scott, *Fuel Cells*, **8**, 453 (2008).
12. S. Tao, *Solid State Ionics*, **180**, 148 (2009).
13. X. Sun, S. Wang, Z. Wang, X. Ye, T. Wen, and F. Huang, *Solid State Ionics*, **179**, 1138 (2008).
14. G. Alberti, M. Casciola, S. Cavalaglio, and R. Vivani, *Solid State Ionics*, **125**, 91 (1999).
15. Y. Li, T. Kunitake, Y. Aoki, and E. Muto, *Adv. Mater.*, **20**, 2398 (2008).
16. P. Heo, H. Shibata, M. Nagao, A. Tomita, T. Hibino, and M. Sano, *J. Electrochem. Soc.*, **153**, A897 (2006).
17. P. Heo, M. Nagao, M. Sano, and T. Hibino, *J. Electrochem. Soc.*, **154**, B53 (2007).
18. P. Heo, M. Nagao, M. Sano, and T. Hibino, *J. Electrochem. Soc.*, **155**, B92 (2008).
19. P. Heo, K. Ito, A. Tomita, and T. Hibino, *Angew. Chem., Int. Ed.*, **47**, 7841 (2008).
20. P. Staiti, M. Minutoli, and S. Hocevar, *J. Power Sources*, **90**, 231 (2000).
21. G. Alberti, M. Casciola, and R. Palombari, *J. Membr. Sci.*, **172**, 233 (2000).
22. J. Kim and I. Honma, *Electrochim. Acta*, **48**, 3633 (2003).
23. D. R. Vernon, F. Meng, S. F. Dec, D. L. Williamson, J. A. Turner, and A. M. Herring, *J. Power Sources*, **139**, 141 (2005).
24. M. Nagai and Y. Chiba, *Solid State Ionics*, **176**, 2991 (2005).
25. J. Kim and B. K. B. Jung, *J. Membr. Sci.*, **207**, 129 (2002).
26. D. M. Tigelaar, J. R. Waldecker, K. M. Peplowski, and J. D. Kinder, *Polymer*, **47**, 4269 (2006).
27. R. C. McDonald, D. W. Gidley, T. Sanderson, and R. S. Vallery, *J. Membr. Sci.*, **332**, 89 (2009).
28. A. Matsuda, T. Kanzaki, Y. Yoshinori, M. Tatsuminago, and T. Minami, *Solid State Ionics*, **139**, 113 (2001).
29. S. Li and M. Liu, *Electrochim. Acta*, **48**, 4271 (2003).
30. V. D. Noto and M. Vittadello, *Electrochim. Acta*, **50**, 3998 (2005).
31. K. M. Petrov, L. M. Kaba, S. Srinivasan, and A. J. Appleby, *Int. J. Hydrogen Energy*, **18**, 377 (1993).